FISEVIER

Contents lists available at ScienceDirect

Colloids and Surfaces A: Physicochemical and Engineering Aspects

journal homepage: www.elsevier.com/locate/colsurfa





Quantification of superhydrophobic functionalization for laser textured metal surfaces

Wuji Huang ^{a,1}, Ramin Ordikhani-Seyedlar ^{b,1}, Avik Samanta ^c, Scott Shaw ^b, Hongtao Ding ^{a,*}

- ^a Department of Mechanical Engineering, University of Iowa, Iowa City, IA 52242, USA
- ^b Department of Chemistry, University of Iowa, Iowa City, IA 52242, USA
- ^c Pacific Northwest National Laboratory, Richland, WA, USA

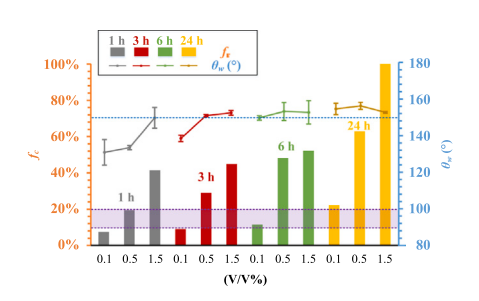
HIGHLIGHTS

- This study constitutes the first attempt to evaluate the effects of chemical immersion treatment for superhydrophobic functionalization of laser textured surfaces.
- A spectroscopic approach is developed to quantitatively measure surface coverage.
- The time and amount of chemicals used in chemical immersion treatment can be reduced dramatically for superhydrophobic metal surfaces.

ARTICLE INFO

Keywords: Laser surface texturing Chemistry modification Metal alloy Superhydrophobic surface Silane solution treatment

GRAPHICAL ABSTRACT



ABSTRACT

Laser texturing is a facile method to promote modified surface wetting properties. While most laser textured metal surfaces are natively superhydrophilic, here we establish a quantitative relationship between post-texturing chemical modification and water contact angles from ca. $80^{\circ} < \theta_{w} < 180^{\circ}$. A nanosecond laser-based high-throughput surface nanostructuring (nHSN) method is used to texture aluminum alloy surfaces. The textured surfaces are immersed in ethanol solutions of chlorosilane reagent [CF₃(CF₂)₅(CH₂)₂SiCl₃] (FOTS) at different concentrations and different times to achieve superhydrophobicity. The role played by the two chemical treatment parameters, concentration and treatment time, is investigated and quantified. Water contact angle, reflection-based infrared spectroscopy and energy-dispersive X-ray spectroscopy are used to characterize the functionalized surface. The goal of this research is to quantify the effects of surface chemical modification on the resulting material functionality using surface sensitive spectroscopic techniques. Our results show that both the solution concentration and the immersion treatment time play significant roles in the attachment of functional groups (-CF₂-, -CF₃) on surface. Further, concentrations of FOTS as low as 0.1% with six hours of chemical immersion treatment, or short treatment times as low as three hours with 0.5% FOTS solution are adequate to achieve superhydrophobicity.

E-mail address: hongtao-ding@uiowa.edu (H. Ding).

^{*} Corresponding author.

¹ These authors contributed equally to this work.

1. Introduction

Laser-based surface texturing techniques have been extensively studied in the past few decades to create superhydrophobic metal and alloy surfaces. Typically, microscale and/or nanoscale surface structures are produced from the laser texturing process. While most textured surfaces are natively superhydrophilic, some can undergo a transition to become superhydrophobic by being exposed to air for a few days to weeks. In order to achieve superhydrophobicity in a more reproducible fashion and shorter period of time, surface chemistry modification method must be performed [1-5]. However, most of the existing literature only reports laser-based texturing processes [6-9] and stresses the types of surface structures created by laser irradiation. In this study, a solution-based treatment method is used to chemically modify the laser-treated surface, inducing superhydrophobicity. The solution concentration and treatment duration are two major parameters that influence the ultimate effect of the chemical treatment. In general, higher concentrations and longer durations lead to more surface modification, enhancing the observed effect. The results presented here use surface sensitive spectroscopies to form, for the first time, a quantitative relationship between these two chemical treatment parameters on the formation of superhydrophobic layers that modify resulting surface wettability of laser-textured surfaces. The influence of the amount of surface-attached carbon-fluorine groups and their spatial distribution on the wettability of the fabricated metal surfaces is evaluated.

Various chemical modification techniques have been implemented to apply superhydrophobic coatings on laser-treated metal surfaces. Among these, extended exposure to ambient air is one of the most popular. During the storage in air, laser textured aluminum surfaces absorb airborne organic molecules that alter the surface chemistry via enrichment of -CH₂- and -CH₃ groups which lead to superhydrophobicity [10,11]. While resource-friendly, this method is time-consuming, requiring as much as two weeks' exposure in air for the surface wettability to achieve superhydrophobicity. Another shortcoming of the air exposure method is that it is difficult to control. Studies have shown that laser processing environments could influence the following wettability transition rate [10,12]. Temperature also influences the wettability transition, as low heat treatments have been shown to accelerate the organic molecular adsorption from air, enhancing superhydrophobicity [13]. Meanwhile, thermal annealing can partially remove the adsorbed organic compounds, leading to hydrophilicity [14].

Other techniques used to achieve superhydrophobicity include attaching low-energy, long-chain, fluorosilane molecules with -CF2- and -CF₃ groups. Here, chemical vapor deposition (CVD) is commonly used. Jagdheesh et al. [15] used ultraviolet laser pulses to generate micro- and nano-roughness features on stainless steel and Ti-6Al-4V sheets, and then created hydrophobic self-assembled monolayers (SAM) by depositing perfluorinated octyl trichlorosilane (FOTS) via CVD. Kam et al. [16] applied a functionalized silane coating (tridecafluoro-1,1,2,2,-tetrahydrooctyl-1-trichlorosilane) via a CVD process on an already hydrophobic surface created by laser irradiation, to further enhance its hydrophobicity. Though commonly applied, the CVD process usually involves higher temperature and hazardous precursors. In comparison, solution-based immersion treatment is an easier way to make superhydrophobic surface. Yang et al. [17] immersed the laser-ablated aluminum samples into (heptadecafluoro-1, 1, 2, 2-tetradecyl) triethoxysilane/ethanol solution for two hours to reduce surface free energy and to achieve superhydrophobicity. Rajab et al. [18] followed a similar procedure by immersion treatment of laser-treated stainless steel samfor two hours using a 1% heptadecafluoro-1,1,2, 2-tetrahydro-decyl-1-trimethoxysilane [CF₃(CF₂)₇(CH₂)₂Si(OCH₃)₃] methanol solution to make stable superhydrophobic surface. In these studies, researchers mainly focused on studying the effect of laser treatment on surface structure and consequent surface wettability, holding the chemical surface treatment parameters constant. By

selecting a nominal concentration (1% \sim 1.5%) and treatment time (2–3 h) for the surface modifying agents, the prior research largely neglects the influence of chemical treatment parameters on surface wetting behaviors.

The lack of studies for chemical treatments of laser-based superhydrophobic metal surfaces motivates our present work, in which we report quantitative analysis of the surface functional groups after chemical modification at varying concentrations and durations. One of the most mature and effectively used technologies to investigate surface chemistry is Fourier transform infrared spectroscopy (FTIR), which is a powerful tool used for decades to assess functional groups deposited on solid surfaces [19], particularly for self-assembled monolayers [20]. Controlling the polarization of the infrared light increases sensitivity, and polarization modulated infrared reflection spectroscopy (PM-IR-RAS) has been used widely in surface chemical analysis for (sub) monolayer systems for decades [21]. More relevant to our current work is a report by Lee et al. [22] that used PM-IRRAS to investigate surface properties of self-assembled monolayers with partially fluorinated tail groups. However, PM-IRRAS is not inherently quantitative, and Lee's study only qualitatively identified the functional groups and surface behaviors. There was no quantitative study being conducted to determine the amount of certain chemical groups.

X-ray Photoelectron Spectroscopy (XPS) and Energy-Dispersive Spectroscopy (EDS) are the other quantitative surface analytical techniques which provide information on the elemental composition information of surface. Wei et al. [23] used XPS to quantify the content of fluorine on a plasma-treated polyethersulfone membrane surfaces. A strong fluorination effect was observed when measuring hydrophobicity induced by increasing the content of fluorine on the surface. Fischer et al. [24] also used EDS to quantify functional group density of silane monolayers made by vapor deposition. In addition, Lu et al. [25] demonstrated that atomic-scale chemical composition across oxide LSMO/BFO interfaces can be quantified using Gaussian peak fitting of EDS profiles. Despite these techniques available to characterize the surface chemical composition, there remains limited research on chemically modified laser-textured metal surface. Therefore, it is necessary to apply the surface characterization techniques to quantitatively investigate the functional groups present on laser-treated metal surfaces.

In our current work, nHSN treated aluminum alloy (AA 6061) samples were immersed in a chlorosilane reagent solution. In the solution stage, chlorine atoms from the chlorosilane induce chemical etching and attachment of the functional group, concurrently [26–28]. As a result, the generation of surface nanostructure and surface chemistry happens simultaneously. We systematically alter the silane reagent concentration (V/V%) as well as the chemical immersion treatment time (T_t) to study the influence of these two chemical treatment variables on the surface attachment of silane molecules and the resultant surface functionality. The quantity and distribution of -CF₂- and -CF₃ functional groups on the surfaces are investigated using PM-IRRAS and EDS analysis. The PM-IRRAS data are quantified by standardizing the arbitrary PM units with separate measurements of known samples by p-polarized IRRAS.

2. Materials and methods

Superhydrophobic surface was made on aluminum alloy (AA 6061) using laser treatment coupled with chemical functionalization method, also termed as nHSN process [26,27]. A Q-switched Nd:YAG nanosecond laser with wavelength of 1064 nm, which emits a pulse duration of 6–8 ns and a pulse energy on the order of hundreds of mJ, was used for laser texturing step. During laser scanning, the aluminum samples were submerged in deionized water, thereby confining the laser-induced plasma and surface-enhancing effects [29,30]. Other details of the laser process can be found in Supporting information S1. After the laser texturing process, the chemical immersion treatment was performed. The laser-textured samples were immersed in ethanol solutions of

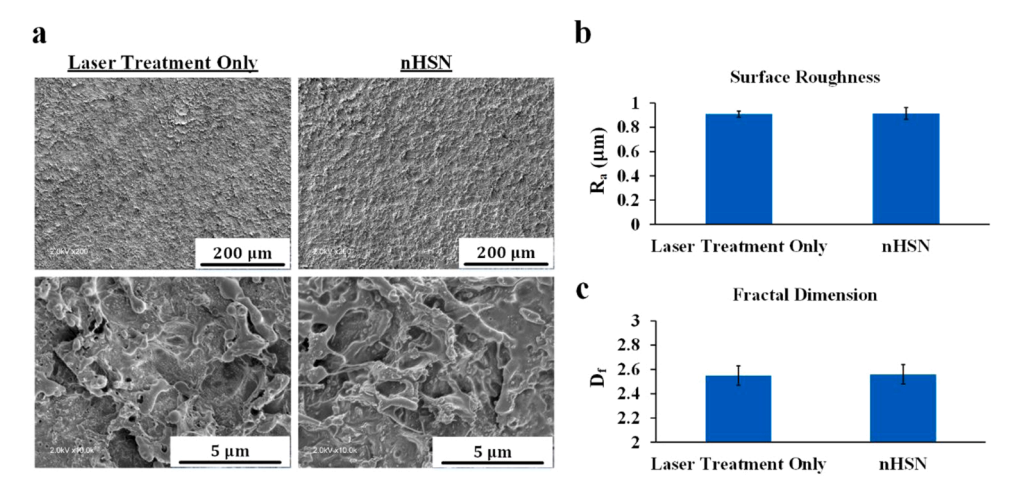


Fig. 1. (a) SEM images of AA6061 laser-treated surfaces with and without chemical immersion treatment. (b) Comparison of surface roughness with (nHSN) and without chemical treatment. (c) Fractal dimension of surfaces with and without chemical treatment.

chlorosilane reagent $[CF_3(CF_2)_5(CH_2)_2SiCl_3]$ (FOTS) with different volume percentage (0.1%, 0.5%, 1.5%), for different time to achieve various wettability.

Morphology of the laser-irradiated and chemical treated rough samples were analyzed using scanning electron microscopy (SEM; Hitachi S-4800). Functional groups on surface were identified and quantitatively studied using PM-IRRAS. EDS was used to determine the chemical elements present in the samples and was used to estimate their relative abundance and spatial distribution. Water contact angle θ_w for the treated specimen surface was measured using a contact angle goniometer (Rame-Hartmodel 100) coupled with a high-resolution CMOS camera (6–60× magnification, Thor Laboratories). For each θ_w measurement, about 5 μ L volume of water was dropped onto the specimen surface to form a still water droplet, and its optical shadowgraph was obtained using the CMOS camera. The resulting image was processed in ImageJ to retrieve the contact angle. Multiple θ_w measurements were performed at various locations of each specimen surface and error bars are reported at 95% confidence intervals.

Surface functional groups were identified and quantitatively studied using PM-IRRAS, which is an established analytical technique for the characterization of thin films on metal surfaces [31,32]. The technique is based on the different absorption of s- and p-polarized infrared light by the surface, modifying film, and surrounding isotropic bulk phase. A differential reflectance spectrum is generated using the following

equation [21,33,34]:

$$\frac{\Delta R}{R} = \frac{Ip - Is}{Ip + Is} \tag{1}$$

Where I_p is the spectrum obtained from the p-polarized light and I_s from s-polarized light. The major advantage of PM-IRRAS technique is its ability to eliminate absorptions caused by atmospheric water vapor and $\rm CO_2$. It allows relatively fast acquisition across the entire mid-infrared range (800–4000 cm⁻¹). While not inherently quantitative, we have calibrated our spectrometer to allow conversion of PMIRRAS intensity units to standard absorbance which permits us to estimate film thicknesses (see details in supporting information S2).

3. Results and discussion

Surface morphology of an aluminum alloy (AA6061) is shown by SEM images at two relevant magnifications in Fig. 1a. The laser-treated surface is random and featureless before (left) and after chemical treatment (right). There is no visible difference in microstructure of the surface (200 micrometer scale bar). In nanoscale images (5 micrometer scale bar), the surface topography appears slightly changed after the chemical immersion treatment (1.5% FOTS for 24 h). However, the visible change is subtle and there is no statistical difference in the surface roughness or fractal dimension as shown in Fig. 1(b),(c). The fractal

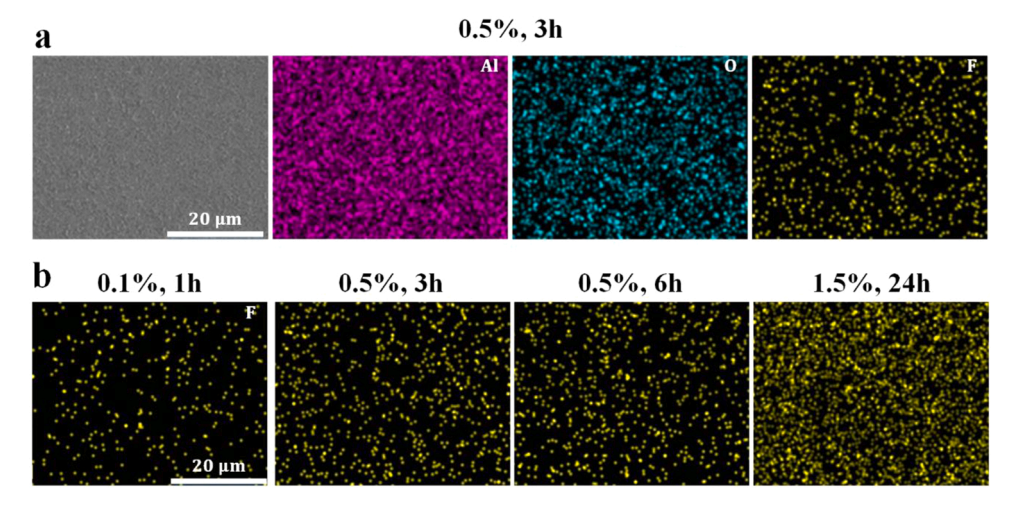
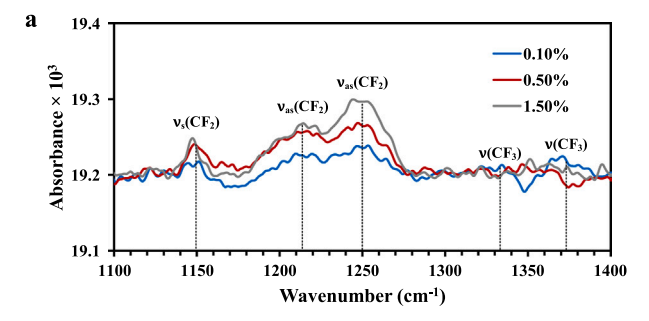
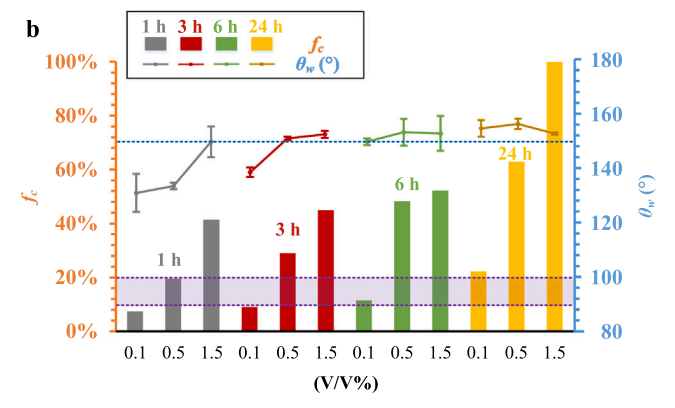


Fig. 2. (a) SEM image and EDS maps of aluminum, oxygen, and fluorine on AA6061 surface treated by 0.5% FOTS for 3 h. (b) EDS maps of fluorine on different AA6061 surfaces treated with varying solution concentrations over varying durations.





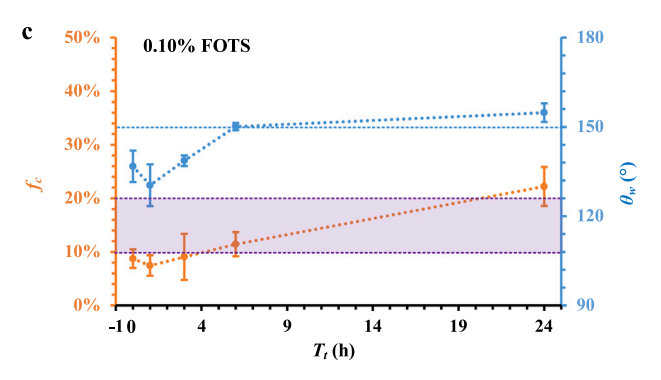


Fig. 3. (a) PM-IRRAS spectra of samples chemically treated with varying solution concentrations for three hours. (b) Relative surface coverage f_c of FOTS on AA6061 surfaces treated with varying solution concentrations for varying treatment time T_b and their corresponding θ_w . (c) Relative surface coverage of FOTS on AA6061 surfaces treated with 0.1% FOTS solution for 10 s, 1 h, 3 h, 6 h and 24 h, and the corresponding θ_w .

dimension is a ratio providing a statistical index of complexity related to surface structures [28,35,36]. Because there is no significant difference in surface morphology before or after the chemical immersion, we focused on the influence of surface chemistry on surface wettability.

After deposition of FOTS, the surface elemental composition was examined by EDS. Fig. 2a shows the EDS maps of Al, O, and F, respectively, collected from the surface treated by 0.5% FOTS solution for 3 h. The oxygen species distribute almost uniformly over the surface, which is in accordance with the oxide and hydroxide generated from the reaction between aluminum with atmospheric oxygen and water at room temperature [37,38]. The distribution of fluorine appears more localized, which indicates higher concentrations of the (-CF₂- and -CF₃) functional groups anchored in some facets of the textured metal surface. Fig. 2b shows the EDS maps of fluorine for samples under various treatment conditions. The amount of fluorine-related intensity generally increases with solution concentration and treatment time. However, because the sample surfaces are rough (feature size is much larger than the wavelength on incident or exiting radiation for EDS), the micro-asperities have induced significant interference and error in

Table 1
Assignment of IR Bands in Fig. 2a [39].

Stretch	Wavenumber (cm ⁻¹)
$ \nu(\text{CF}_3) $ $ \nu_{as}(\text{CF}_2) $ $ \nu_s(\text{CF}_2)$	1372, 1333 1250, 1214 1153

 ν_s = symmetric stretch; ν_{as} = antisymmetric stretch.

quantitative analysis. Therefore, EDS measurements have reduced precision. We believe this effect contributes to the localized 'spots' of fluorine on the surface, masking fluorine signals from adjacent areas. While qualitatively useful, we turn to PM-IRRAS for more accurate and quantitative analysis of the surface chemistry.

The characteristic vibrational frequencies and intensities of the modified surface were studied by PM-IRRAS. Fig. 3a shows a series of PM-IRRAS spectra from 1100 cm⁻¹ to 1400 cm⁻¹ for three surfaces exposed to different concentrations of the FOTS solution. The PM-IRRAS spectral intensity is expressed as a ratio computed by the intensities of reflected p- and s-polarized light [37]. In order to quantify functional groups on the surface, we applied a Beer's Law type analysis, using alkanethiol coated substrates as references to standardize the otherwise arbitrary PMIRRAS intensity values. For details on this process, see Supporting information S3. The absorption peaks are assigned to the symmetric and antisymmetric stretches of -CF₂- and -CF₃, accordingly, as listed in Table 1 [39]. The most intense peak, at 1250 cm⁻¹, is assigned to the asymmetric stretch (ν_{as}) of -CF₂-. The ν_{as} (CF₂) peak intensities correlate with the amount of FOTS in the deposition solution, indicating that higher concentrations of deposition solution result in more FOTS deposition. For example, the substrate from 0.1% FOTS solution shows the lowest peak intensities, and the samples treated with 1.5% FOTS solution show the highest peak intensities. The peak intensity increases with the solution concentration, and we used this relationship to quantify the amount of -CF2- functional groups present on the different surfaces.

Ultimately, the relationships between relative surface coverage (f_c) , contact angle (θ_w) , and the deposition conditions are shown in Fig. 3b. The added roughness of the laser textured surfaces used here results in the low relative surface coverage of the samples treated by low concentration (0.1% and 0.5%) of FOTS solution for short durations (1 h, 3 h, and 6 h). Based on significant literature precedence [40-45], it is safe to say that the sample treated with 1.5% solution for 24 h has 100% relative surface coverage of FOTS. The increasing f_c and increasing hydrophobicity of the surfaces with the increase of solution concentration and T_t is clearly seen by measuring the contact angle of water shown as blue dots in Fig. 3b. In addition, the purple band indicates the transitional region between the superhydrophobicity and hydrophobicity. The superhydrophobicity will be achieved when the f_c is greater than 20%, while f_c lower than around 10% will lead to hydrophobicity. When f_c falls between 10% and 20%, the surface is on a transition stage from hydrophobicity to superhydrophobicity, where the surface wettability is to be determined on a case-by-case basis. Correspondingly, the immersion treatment with 0.1% FOTS solution for 6 h can induce superhydrophobicity. When the solution concentration is increased to 0.5%, it takes only 3 h to achieve superhydrophobicity.

Fig. 3c shows the relationship between f_c , θ_w and the T_t for surfaces treated with 0.1% solution. It is found that a quick formation of FOTS surface layer happened in the first 10 s followed by a 24 h slow accretion, indicating that the process of FOTS layer formation on certain area (valley) of AA6061 surface is fast and energetically favorable, while it takes longer time for FOTS molecules to be deposited onto the other area (mountain top) [46]. And it is these remaining sites that play the most important role in determining the surface wettability. The surface becomes superhydrophobic when f_c reaches 20%.

4. Conclusions

The research shows a strong relationship between the solution concentration, chemical treatment time, and the water contact angle on the superhydrophobic metal surface. Specifically, the surface selective, quantitative analysis used in this research clearly shows that different surface coverages as a function of FOTS concentration in ethanol solutions. The results indicate that the FOTS deposition on textured AA6061 surfaces occurs rapidly on some surface sites (presumably those in the 'valleys' of the texturing), while the rest of the surface sites are covered more slowly particularly at the lower solution concentrations of FOTS. Importantly, these remaining surface sites appear to have the most significant effect on controlling the water contact angle/surface hydrophobicity. Precisely, the relative surface coverage of FOTS greater than 20% leads to superhydrophobicity, while surface coverage lower than 10% results in hydrophobicity for laser textured surfaces. From an engineering point of view, chemical immersion in ethanol solution of 0.1 V/V% FOTS in ethanol for six hours assures superhydrophobicity. When the concentration of FOTS is increased to 0.5%, it takes only three hours to achieve superhydrophobicity. Lower FOTS concentrations or treatment time will not guarantee enough saturation of -CF₂- and -CF₃ functional groups on aluminum surface, leading to weaker superhydrophobicity (less than 150° of water contact angle). The results provided here could be used to explain results of prior papers that use textured surfaces and modifying chemical adsorbates and as a guide making reproducibly superhydrophobic metal surfaces. Compared with traditional chemical treatment methods, these results show that shorter chemical immersion treatment times and lower chemical solution concentrations (three hours for FOTS concentration of 0.5 V/V% and six hours for lower FOTS concentration of 0.1 V/V%) are sufficient to achieve superhydrophobicity.

CRediT authorship contribution statement

W. Huang performed the nHSN experiments and surface topography characterizations. R. Ordikhani-Seyedlar conducted the EDS and PM-IRRAS analyses for this study. W. Huang and R. Ordikhani-Seyedlar composed the manuscript and contributed equally to this work. A. Samanta helped with the experimental analysis. S. K. Shaw contributed to the chemical analysis aspects of the investigation. H. Ding developed the theoretical concepts and supervised the investigation. S. K. Shaw and H. Ding revised and finalized the manuscript. All participants discussed the results and commented on the manuscript.

Declaration of Competing Interest

The authors declare that they have no known competing financial interests or personal relationships that could have appeared to influence the work reported in this paper.

Acknowledgments

The authors gratefully acknowledge the financial support by the National Science Foundation under Grant Number CMMI-1762353.

Appendix A. Supporting information

Supplementary data associated with this article can be found in the online version at doi:10.1016/j.colsurfa.2021.128126.

References

[1] B. jia Li, H. Li, L. jing Huang, N. fei Ren, X. Kong, Femtosecond pulsed laser textured titanium surfaces with stable superhydrophilicity and superhydrophobicity, Appl. Surf. Sci. 389 (2016) 585–593, https://doi.org/ 10.1016/j.apsusc.2016.07.137.

- [2] R. Jagdheesh, Fabrication of a superhydrophobic Al2O3 surface using picosecond laser pulses, Langmuir 30 (2014) 12067–12073, https://doi.org/10.1021/ hsp03257
- [3] C.-V. Ngo, D.-M. Chun, Fast wettability transition from hydrophilic to superhydrophobic laser-textured stainless steel surfaces under low-temperature annealing, Appl. Surf. Sci. 409 (2017) 232–240, https://doi.org/10.1016/j. applies 2017 03 038
- [4] A. Samanta, Q. Wang, S.K. Shaw, H. Ding, Roles of chemistry modification for laser textured metal alloys to achieve extreme surface wetting behaviors, Mater. Des. 192 (2020), 108744, https://doi.org/10.1016/j.matdes.2020.108744.
- [5] A. Samanta, W. Huang, H. Chaudhry, Q. Wang, S.K. Shaw, H. Ding, Design of chemical surface treatment for laser-textured metal alloys to achieve extreme wetting behavior, ACS Appl. Mater. Interfaces 12 (2020) 18032–18045, https:// doi.org/10.1021/acsami.9b21438.
- [6] A. Milionis, E. Loth, I.S. Bayer, Recent advances in the mechanical durability of superhydrophobic materials, Adv. Colloid Interface Sci. 229 (2016) 57–79, https:// doi.org/10.1016/j.cis.2015.12.007.
- [7] J. Jeevahan, M. Chandrasekaran, G. Britto Joseph, R.B. Durairaj, G. Mageshwaran, Superhydrophobic surfaces: a review on fundamentals, applications, and challenges, J. Coat. Technol. Res. 15 (2018) 231–250, https://doi.org/10.1007/ s11998-017-0011-x.
- [8] X. Feng, L. Jiang, Design and creation of superwetting/antiwetting surfaces, Adv. Mater. 18 (2006) 3063–3078, https://doi.org/10.1002/adma.200501961.
- [9] F. Chen, D. Zhang, Q. Yang, J. Yong, G. Du, J. Si, F. Yun, X. Hou, Bioinspired wetting surface via laser microfabrication, ACS Appl. Mater. Interfaces 5 (2013) 6777–6792, https://doi.org/10.1021/am401677z.
- [10] J. Long, M. Zhong, H. Zhang, P. Fan, Superhydrophilicity to superhydrophobicity transition of picosecond laser microstructured aluminum in ambient air, J. Colloid Interface Sci. 441 (2015) 1–9, https://doi.org/10.1016/j.jcis.2014.11.015.
- [11] P. Bizi-Bandoki, S. Valette, E. Audouard, S. Benayoun, Time dependency of the hydrophilicity and hydrophobicity of metallic alloys subjected to femtosecond laser irradiations, Appl. Surf. Sci. 273 (2013) 399–407, https://doi.org/10.1016/j. apuse 2013.02.054
- [12] P. Pou, J. del Val, A. Riveiro, R. Comesaña, F. Arias-González, F. Lusquiños, M. Bountinguiza, F. Quintero, J. Pou, Laser texturing of stainless steel under different processing atmospheres: From superhydrophilic to superhydrophobic surfaces, Appl. Surf. Sci. 475 (2019) 896–905, https://doi.org/10.1016/j.apsusc.2018.12.248.
- [13] C.V. Ngo, D.M. Chun, Effect of heat treatment temperature on the wettability transition from hydrophilic to superhydrophobic on laser-ablated metallic surfaces, Adv. Eng. Mater. 20 (2018) 1–11, https://doi.org/10.1002/adem.201701086.
- [14] Z. Yang, X. Liu, Y. Tian, Insights into the wettability transition of nanosecond laser ablated surface under ambient air exposure, J. Colloid Interface Sci. 533 (2019) 268–277.
- [15] R. Jagdheesh, B. Pathiraj, E. Karatay, G.R.B.E. Römer, A.J. Huis In'T Veld, Laser-induced nanoscale superhydrophobic structures on metal surfaces, Langmuir 27 (2011) 8464–8469, https://doi.org/10.1021/la2011088.
- [16] D.H. Kam, S. Bhattacharya, J. Mazumder, Control of the wetting properties of an AISI 316L stainless steel surface by femtosecond laser-induced surface modification, J. Micromech. Microeng. 22 (2012), 105019, https://doi.org/ 10.1088/0960-1317/22/10/105019.
- [17] Z. Yang, X. Liu, Y. Tian, Hybrid laser ablation and chemical modification for fast fabrication of bio-inspired super-hydrophobic surface with excellent self-cleaning, stability and corrosion resistance, J. Bionic Eng. 16 (2019) 13–26, https://doi.org/ 10.1007/s42235-019-0002-y.
- [18] F.H. Rajab, Z. Liu, L. Li, Long term superhydrophobic and hybrid superhydrophobic/superhydrophilic surfaces produced by laser surface micro/ nano surface structuring, Appl. Surf. Sci. 466 (2019) 808–821, https://doi.org/ 10.1016/j.apsusc.2018.10.099.
- [19] H. Seki, K. Kunimatsu, W.G. Golden, A thin-layer electrochemical cell for infrared spectroscopic measurements of the electrode/electrolyte interface, Appl. Spectrosc. 39 (1985) 437–443.
- [20] P.E. Laibinis, G.M. Whitesides, D.L. Aliara, Y.T. Tao, A.N. Parikh, R.G. Nuzzo, Comparison of the structures and wetting properties of self-assembled monolayers of n-alkanethiols on the coinage metal surfaces, Cu, Ag, Au, J. Am. Chem. Soc. 113 (1991) 7152–7167, https://doi.org/10.1021/ja00019a011.
- [21] B.J. Barner, M.J. Green, E.I. Sáez, R.M. Corn, Polarization modulation fourier transform infrared reflectance measurements of thin films and monolayers at metal surfaces utilizing real-time sampling electronics, Anal. Chem. 63 (1991) 55–60, https://doi.org/10.1021/ac00001a010.
- [22] H. Fukushima, S. Seki, T. Nishikawa, H. Takiguchi, K. Tamada, K. Abe, R. Colorado, M. Graupe, O.E. Shmakova, T.R. Lee, Microstructure, wettability, and thermal stability of semifluorinated self-assembled monolayers (SAMs) on gold, J. Phys. Chem. B 104 (2000) 7417–7423.
- [23] X. Wei, B. Zhao, X.-M. Li, Z. Wang, B.-Q. He, T. He, B. Jiang, CF4 plasma surface modification of asymmetric hydrophilic polyethersulfone membranes for direct contact membrane distillation, J. Memb. Sci. 407–408 (2012) 164–175, https:// doi.org/10.1016/j.memsci.2012.03.031.
- [24] T. Fischer, P.M. Dietrich, C. Streeck, S. Ray, A. Nutsch, A. Shard, B. Beckhoff, W.E. S. Unger, K. Rurack, Quantification of variable functional-group densities of mixed-silane monolayers on surfaces via a dual-mode fluorescence and XPS label, Anal. Chem. 87 (2015) 2685–2692, https://doi.org/10.1021/ac503850f.
- [25] P. Lu, J. Xiong, M. Van Benthem, Q. Jia, Atomic-scale chemical quantification of oxide interfaces using energy-dispersive X-ray spectroscopy, Appl. Phys. Lett. 102 (2013), https://doi.org/10.1063/1.4804184.

- [26] A. Samanta, Q. Wang, S.K. Shaw, H. Ding, Nanostructuring of laser textured surface to achieve superhydrophobicity on engineering metal surface, J. Laser Appl. 31 (2019), 022515, https://doi.org/10.2351/1.5096148.
- [27] Q. Wang, A. Samanta, S.K. Shaw, H. Hu, H. Ding, Nanosecond laser-based high-throughput surface nanostructuring (nHSN), Appl. Surf. Sci. 507 (2020), 145136, https://doi.org/10.1016/j.apsusc.2019.145136.
- [28] A. Samanta, W. Huang, M. Bell, S.K. Shaw, N. Charipar, H. Ding, Large-area surface wettability patterning of metal alloys via a maskless laser-assisted functionalization method, Appl. Surf. Sci. 568 (2021), 150788, https://doi.org/10.1016/J. APSUSC.2021.150788.
- [29] N. Shen, H. Ding, Q. Wang, H. Ding, Effect of confinement on surface modification for laser peen forming without protective coating, Surf. Coat. Technol. 289 (2016), https://doi.org/10.1016/j.surfcoat.2016.01.054.
- [30] N. Shen, H. Ding, R. Bowers, Y. Yu, C.N. Pence, I.T. Ozbolat, C.M. Stanford, Surface micropatterning of pure titanium for biomedical applications via high energy pulse laser peening, J. Micro Nano-Manuf. 3 (2014), 011005, https://doi.org/10.1115/ 14020247
- [31] D. Blaudez, S. Castano, B. Desbat, PM-IRRAS at liquid interfaces, in: Biointerface Characterization by Advanced IR Spectroscopy, Elsevier, 2011, pp. 27–55.
- [32] V. Zamlynny, J. Lipkowski, Quantitative SNIFTIRS and PM IRRAS of organic molecules at electrode surfaces, Adv. Electrochem. Sci. Eng. 9 (2006) 315.
- [33] W.N. Hansen, Electric fields produced by the propagation of plane coherent electromagnetic radiation in a stratified medium, JOSA 58 (1968) 380–390.
- [34] A.S. Ichimura, W. Lew, D.L. Allara, Tripod self-assembled monolayer on au(111) prepared by reaction of hydroxyl-terminated alkylthiols with SiCl4, Langmuir 24 (2008) 2487–2493, https://doi.org/10.1021/la703196b.
- [35] J.I. Rosales-Leal, M.A. Rodríguez-Valverde, G. Mazzaglia, P.J. Ramón-Torregrosa, L. Díaz-Rodríguez, O. García-Martínez, M. Vallecillo-Capilla, C. Ruiz, M. A. Cabrerizo-Vílchez, Effect of roughness, wettability and morphology of engineered titanium surfaces on osteoblast-like cell adhesion, Colloids Surf. A Physicochem. Eng. Asp. 365 (2010) 222–229, https://doi.org/10.1016/j.colsurfa.2009.12.017.
- [36] W. Huang, A. Samanta, Y. Chen, S. Baek, S.K. Shaw, H. Ding, Machine learning model for understanding laser superhydrophobic surface functionalization, J. Manuf. Process. 69 (2021) 491–502, https://doi.org/10.1016/J. JMAPRO.2021.08.007.

- [37] Z. Deng, Y. Liu, Y. Tanaka, H. Zhang, J. Ye, Y. Kagawa, Temperature effect on hydrogen generation by the reaction of γ-Al2O3–modified Al powder with distilled water, J. Am. Ceram. Soc. 88 (2005) 2975–2977.
- [38] Z. Deng, Y. Liu, Y. Tanaka, J. Ye, Y. Sakka, Modification of Al particle surfaces by γ-Al2O3 and its effect on the corrosion behavior of Al, J. Am. Ceram. Soc. 88 (2005) 977–979.
- [39] Y. Ren, K.I. Iimura, A. Ogawa, T. Kato, Surface micelles of CF3(CF2)7(CH2) 10COOH on aqueous La3+ subphase investigated by atomic force microscopy and infrared spectroscopy, J. Phys. Chem. B 105 (2001) 4305–4312, https://doi.org/10.1021/jp004502a.
- [40] U. Srinivasan, M.R. Houston, R.T. Howe, R. Maboudian, Alkyltrichlorosilane-based self-assembled monolayer films for stiction reduction in silicon micromachines, J. Micro Syst. 7 (1998) 252–259, https://doi.org/10.1109/84.679393.
- [41] L. Sang, K.M. Knesting, A. Bulusu, A.K. Sigdel, A.J. Giordano, S.R. Marder, J. J. Berry, S. Graham, D.S. Ginger, J.E. Pemberton, Effect of time and deposition method on quality of phosphonic acid modifier self-assembled monolayers on indium zinc oxide, Appl. Surf. Sci. 389 (2016) 190–198, https://doi.org/10.1016/j.apsusc.2016.06.183.
- [42] R. Banga, J. Yarwood, A.M. Morgan, B. Evans, J. Kells, FTIR and AFM studies of the kinetics and self-assembly of alkyltrichlorosilanes and (Perfluoroalkyl) trichlorosilanes onto glass and silicon, Langmuir 11 (1995) 4393–4399, https:// doi.org/10.1021/la00011a036.
- [43] J. Xiang, P. Zhu, Y. Masuda, K. Koumoto, Fabrication of Self-Assembled Monolayers (SAMs) and inorganic micropattern on flexible polymer substrate, Langmuir 20 (2004) 3278–3283, https://doi.org/10.1021/la036088m.
- [44] A.G. Richter, M.K. Durbin, C.J. Yu, P. Dutta, In situ time-resolved X-ray reflectivity study of self-assembly from solution, Langmuir 14 (1998) 5980–5983, https://doi. org/10.1021/la980371h.
- [45] D. Appelhans, D. Ferse, H.J.P. Adler, W. Plieth, A. Fikus, K. Grundke, F.J. Schmitt, T. Bayer, B. Adolphi, Self-assembled monolayers prepared from ω-thiophenefunctionalized n- alkyltrichlorosilane on silicon substrates, Colloids Surf. A Physicochem. Eng. Asp. 161 (2000) 203–212, https://doi.org/10.1016/S0927-7757(99)00338-6.
- [46] J.I. Iribarren-Mateos, I. Buj-Corral, J. Vivancos-Calvet, C. Alemán, J.I. Iribarren, E. Armelin, Silane and epoxy coatings: a bilayer system to protect AA2024 alloy, Prog. Org. Coat. 81 (2015) 47–57, https://doi.org/10.1016/j. porccoat.2014.12.014.